3.1 Process Development and Optimization for Silicon Carbide Joining and Irradiation Studies-III — T. Koyanagi, J. Kiggans, C. Shih, Y. Katoh (Oak Ridge National Laboratory)

OBJECTIVE

The objective of this task is to develop and optimize joining processes for silicon carbide (SiC) ceramics and composites for fusion energy applications.

SUMMARY

Two robust pressureless joining methods for SiC ceramics proved to be promising. A Ti-Si-C MAX phase displacement reaction bonding using commercial bonding formula demonstrated dense microstructures and apparent shear strength of ~150 MPa. A pressureless transient eutectic-phase (TEP) process was newly developed to demonstrate promising properties. An experimental plan for the neutron irradiation effects study was developed.

PROGRESS AND STATUS

Introduction

Development of SiC joints that retain adequate mechanical and functional properties in fusion reactor environment is essential for use SiC and its composites as the primary structural material [1]. Requirement of external pressurization during joining process is a major factor that dictates applicability of a specific joining method to integration of components with certain geometries and dimensions. While several joining technologies for SiC ceramics and composites have proved to be neutron irradiation tolerant to low-to-intermediate fluence levels in our previous study [2], all the joining processes involved require substantial pressurization with an exception of the calcia-alumina glass-ceramic joining. The present work focuses on development of processes that are anticipated to be radiation-tolerant but do not require external pressurization for joining SiC ceramics and composites.

In the previous report [3], the optimal processing conditions for Ti and Mo foil joining have been established. In the present work, pressure-less Ti-Si-C MAX phase joining and pressure-less TEP joining were specifically prepared and evaluated. The Ti-Si-C MAX phase joining was chosen because of the previously demonstrated neutron tolerance for a similar joint, relatively low processing temperature requirement, and availability of commercial joining material. The TEP joining was considered particularly attractive because of its ability to produce SiC-based bond that anticipated leads to robust strength and irradiation tolerance.

Neutron irradiation can affect the physical and mechanical properties of the SiC joints, and the irradiation effects are of critical importance in reactor technology. This report also provides an updated technical plan for the neutron irradiation experiment in the High Flux Isotope Reactor (HFIR).

Experimental Procedure

Materials

For MAX phase bonding, a set of joining agent materials were purchased from Hyper-Therm High Temperature Composites, Inc. (currently Rolls-Royce High Temperature Composites, Inc., Huntington Beach, CA). Ti_3SiC_2-based joints of CVD SiC were produced at ORNL based on a pressure-less slurry process per the Hyper-Therm formula. Two types of the MAX phase joints were prepared in this work. The process conditions were same among them except for the method of slurry preparation. Details of the raw materials and the process conditions are proprietary.

The TEP joints were formed using four types of mixed powders. The mixed powders consist of SiC nano-powder (average diameters ~30 nm) or combined SiC nano- and micron-powders, and sintering additives (Al_2O_3 powder and Y_2O_3 powder) with or without organic agents. The total amount of the oxide additives was 6 or 10 wt.%. To form the TEP joints, SiC plates sandwiching thin mixed powder were cold-pressed at ~10 MPa and then heat-treated at 1875°C for 1 h in an argon atmosphere. Process conditions determined and the specimen ID are summarized in Table 1.

Table 1. Processing conditions, apparent shear strength, fracture behavior, and joint phases of CVD-SiC joined by MAX phase and TEP methods.

Joining method	**Specimen ID**	**Processing Conditions**				**Joint Strength**			**Phases in joint layer**
		Starting Materials	Atmosphere	Temperature (°C)	Time (h)	DNS Strength (MPa)[2]	Torsion shear strength (MPa)[2]	Fracture location	
MAX Phase	MAX-A	N.A.[1]	N.A.	N.A.	N.A.	141±23	152±16	Joint layer for DNS Substrate for torsion	Ti_3SiC_2, TiC, unknown phase
	MAX-B	N.A.	N.A.	N.A.	N.A.	44±10	142±15	Substrate and joint layer for DNS Substrate for torsion	Expected to be same as MAX-A
TEP	TEP-6A	SiC nano and micron powder, 6wt.% oxide additives, Organic agents	Ar	1875	1	113±52	N.D.[3]	Joint layer	SiC, oxide phases
	TEP-6B	SiC nano powder, 6wt.% oxide additives, Organic agents	Ar	1875	1	163±43	N.D.	Substrate	SiC, oxide phases
	TEP-6C	SiC nano powder, 6wt.% oxide additives,	Ar	1875	1	N.D.	N.D.	N.D.	SiC, oxide phases
	TEP-10B	SiC nano powder, 10wt.% oxide additives, Organic agents	Ar	1875	1	N.D.	N.D.	N.D.	SiC, oxide phases

[1] Not available due to the proprietary
[2] Average strength ±one standard deviation
[3] Not determined

Strength evaluation

Shear strength of the SiC joints were determined by double-notch shear (DNS) test [4] and torsional shear test. The DNS test has advantages for both the ease of specimen preparation and for testing. However, this test cannot provide uniform stress states at the joints, which makes an accurate evaluation of the strength difficult. The torsional shear test using an hourglass specimen is near ideal to evaluate accurate evaluation of the strength because of its ability to apply true shear loading to the joint specimens, but it is relatively difficult to machine the test specimen. Therefore, the DNS test was used for quick estimation of the shear strength and the torsion test was used for accurate strength evaluation in this work.

For DNS test specimen, distance between the notches, the notch width, and curvature radius of the notch tip were 3, 0.5, and 0.2 mm, respectively. The tip of both notches reached the joint layer. The tests were conducted at a constant cross head displacement rate of 0.6 mm/min. More than three DNS tests were conducted for each processing condition. Detailed test procedure can be found elsewhere [4].

The dimensions of the torsional test specimen were 6 mm × 6 mm × 3 mm, and diameter of the neck was 5 mm as shown in Figure 1. The torsional load was applied in a universal testing machine with a wire equipped rotating disk fixture (Figure 2). Aluminum-alloy tabs were installed at the square grip sections to obtain uniform stress distributions there. The crosshead speed was 1.0 mm/min with an estimated rotation speed of about 0.025 rad/min. Nominal shear strength values (τ) in this work are given by following equation,

$$\tau = 16T/\pi d^3 \quad (1)$$

where T is the applied torque and d is the specimen diameter of the neck. Number of the torsion test was more than two for each condition. Further description of details of the test method can be found elsewhere [4]. All mechanical tests were conducted at room temperature.

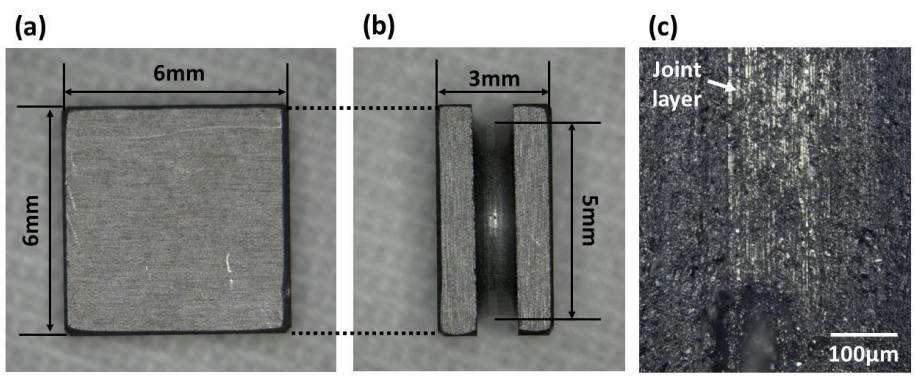

Fig. 1. Optical micrograph of torsional test specimen (MAX-B specimen):
(a) Top-view image, and (b and c) side-view images.

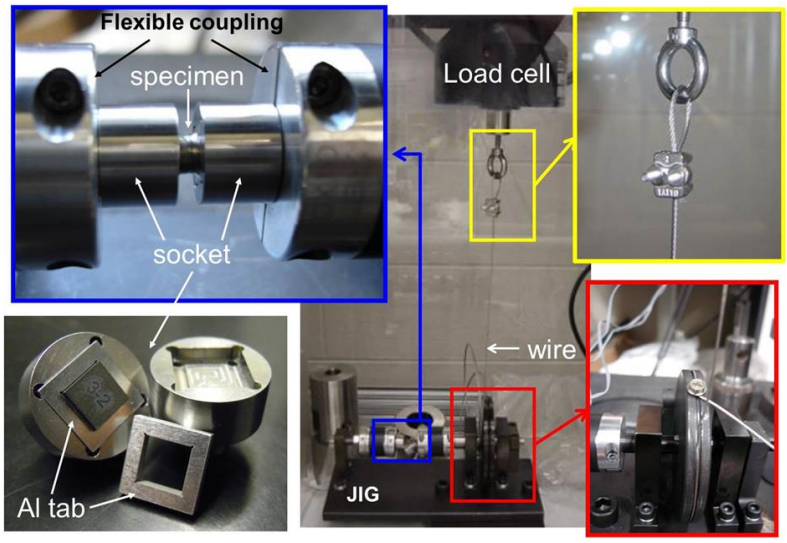

Fig. 2. Overview of the torsional testing machine.

Metallographic examinations

Microstructures of the bonded regions were characterized using optical microscope (Keyence, VHX-1000) and field-emission scanning electron microscope (SEM, Hitachi, S4800) equipped with energy dispersive spectroscopy (EDS). The phases of the joints were determined by XRD analysis (Model Scinatag Pad V, Thermo ARL) on the fracture surface of the DNS specimens.

RESULTS

Pressureless MAX phase joining

Defects in the as-processed joints were observed using the optical microscope as shown in Figure 3. The MAX-A specimen contained high-density pores in the bonded-zone and the joint interface. By contrast, crack roughly perpendicular to the joint boundary was dominant processing defect in the MAX-B specimen.

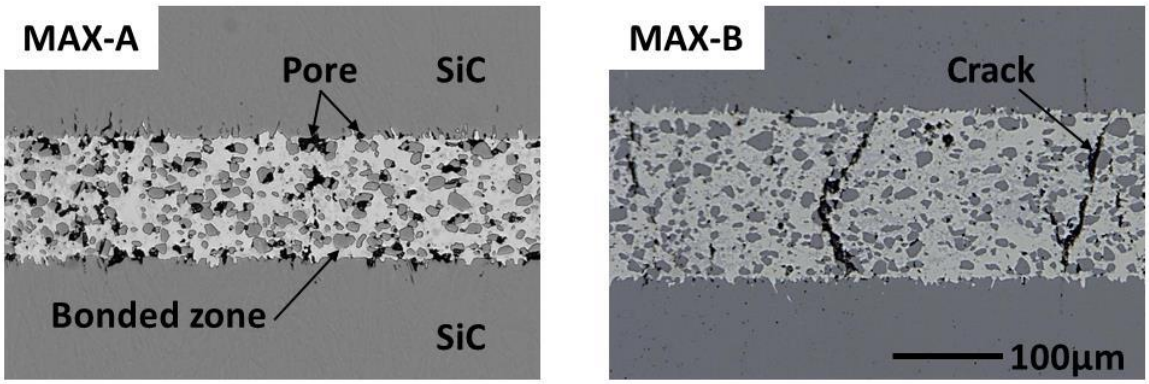

Fig. 3. Optical micrograph of MAX phase jointed SiC.

Analysis using SEM/EDS revealed that the bonded zone of the MAX-A specimen consisted of SiC grains and Ti-Si-C phase as shown in Figure 4(a). Hexagonal Ti_3SiC_2 was the main phase in the Ti-Si-C phase based on SEM/EDS (Figure 4(b)) and XRD analysis. The Ti-Si-C phase also contained cubic TiC and unknown phase. The Ti_3SiC_2 and TiC phases had random grain-orientation based on analysis of the XRD patterns. Note that the EDS spectrum of the point C in Figure 4(b) was affected by both Ti_3SiC_2 and the unknown phase considering the spot size of the SEM. Average atomic number of the unknown phase was higher than Ti_3SiC_2 judging from the backscattered electron image. Therefore, the possible candidates of that phase are TiSi, $TiSi_2$, Ti_5Si_4, and $Ti_5Si_3C_X$, according to the phase diagram of Ti-Si-C system [4].

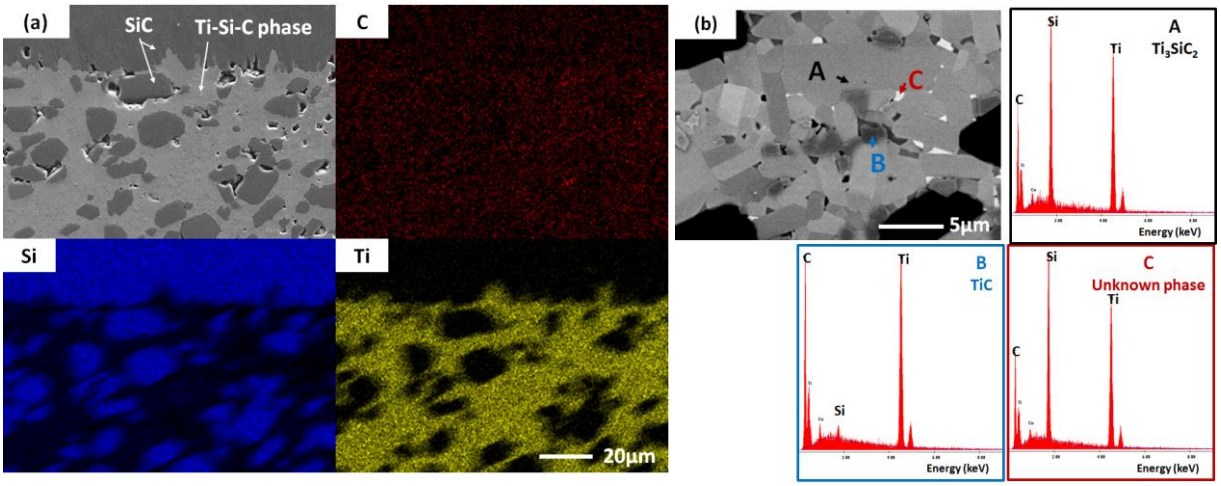

Fig. 4. SEM images and EDS spectra of the MAX-A specimen: (a) secondary electron image, and (b) backscattered electron image.

Figure 5 shows SEM images of the as-fabricated MAX phase joints. Micro-cracks along the grain boundaries were found in both specimens in addition to ~1 micron-sized pores. These cracks may be caused by the misfit strain due to differential coefficients of thermal expansion (CTE) between Ti_3SiC_2 phase (*a*-axis 8.6×10^{-6} K^{-1}, and *c*-axes 9.75×10^{-6} K^{-1} at RT to 906°C [5]) and SiC (4.0×10^{-6} K^{-1} at RT to 1000°C according to material property data sheet from Dow Chemical Co.).

The strong anisotropy of the thermal expansion in the Ti_3SiC_2 phase was also possible cause of the micro cracking at the grain boundaries. Minor phases in Ti-Si-C layer can also affect the strain due to the CTE mismatch.

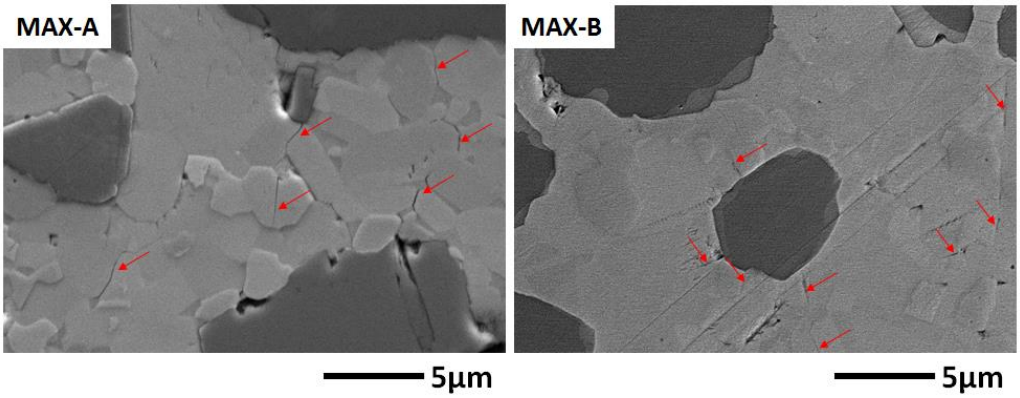

Fig. 5. Secondary electron images of as-fabricated MAX-A and MAX-B specimens. Micro-cracks are arrowed.

The apparent DNS strengths of the MAX phase joined SiC are summarized in Table 1. The average DNS strengths of the MAX-A and MAX-B joints were 141 and 44 MPa, respectively. In addition, the typical fracture appearances of the test specimens are shown in Figure 6. Notch to notch fractures were observed in both specimens. In the MAX-A specimen, the cracks propagated along the joint layer. By contrast, the cracks ran through both the SiC substrates and the joint layer in the MAX-B specimen. This differential fracture behavior may be caused by the differences of the defect shape, size, and the distribution in the bonded zone as shown in Figure 3.

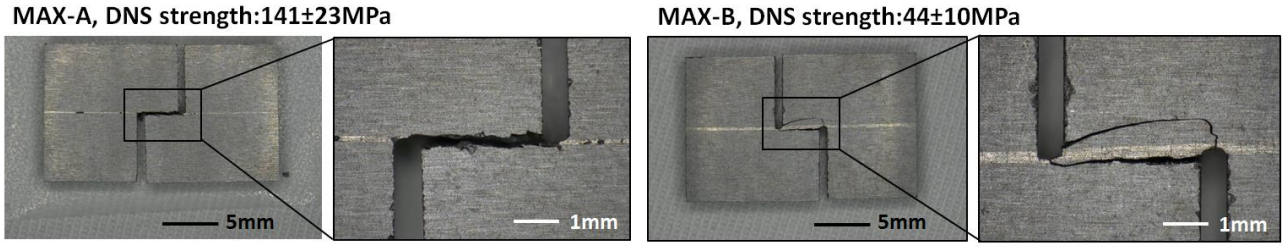

Fig. 6. Typical fracture appearances of MAX phase jointed SiC after DNS tests. The average strength and the one standard deviation are also shown.

Nominal shear strengths of ~150 MPa were demonstrated by the torsional test for both MAX phase jointed specimens. All specimens failed at the SiC substrates as shown in Figure 7, and the fracture appearance was similar between the MAX-A and MAX-B joint specimens. This base failure was typically observed in robust SiC joints determined by the torsional shear test on hourglass specimens [2]. In case of a weak bonding of SiC joints, the flat failure at the joint plane was observed, and the shear strength was typically less than~100 MPa [2, 6]. Therefore, the torsional tests in this work indicate that both MAX phase joints had adequate shear strength. The weak DNS strength of the MAX-B specimen is not considered here, because only the torsional test can give a quantitative strength value as mentioned in the experimental section. It is difficult to identify the location of the crack initiation for the robust joints in the torsion test, because the neck part of the specimen got shattered into pieces after the test. In the torsional test, maximum stress is loaded at the surface of a neck with a minimum diameter, which corresponds to the jointed region in this study. Since machining defects on the specimen surface was more significant comparing to the process defects as shown in Figure 1(c), the fractures in the MAX phase jointed SiC might initiate from the machining defects near the joint layer.

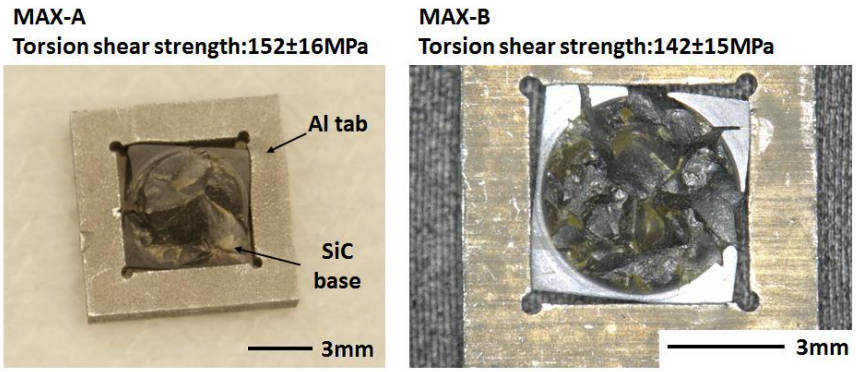

Fig. 7. Micrographs of pieces of the torsional tested specimens for the MAX-A and MAX-B. The average strength and the one standard deviation are also shown.

<u>Pressureless transient eutectic-phase joining</u>

Microstructures of the as-fabricated TEP joined SiC are shown in Figure 8. It is found that the SiC-based joint layers of all specimens were composed of two different regions, where the one is well-sintered region and the other is porous region. The well-sintered regions contained secondary phases attributed to the sintering additives at the grain pockets and grain boundaries, and the secondary phases were rarely observed in the pours region. Effects of type of the starting SiC powder on the microstructures can be seen in SEM images of the TEP-6A fabricated with SiC nano- and micron-powders and TEP-6B with only the SiC nano-powder. Area ratio of the well-sintered region was not significantly different between them, but the size of the pores was smaller in the TEP-6 specimen. The effects of the use of the organic agents were clearly found in the images of the TEP-6B joint with the organic agents and TEP-6C joint without the organic agents. The large pores were observed in the bonded region of the TEP-6C joint. This result strongly indicates that the use of the organic agent was effective for improving the quality of the TEP joint.

The effects on the amount of sintering additives can be seen in the SEM images of the TEP-6B (6 wt.% of additives) joint and TEP-10B (10 wt.% of additives) joint. Reduction of the porosity was achieved by the increased use of the additives. On the other hand, the segregation of the secondary phases at the joint interface and network of the secondary phases became marked with increasing the amount of the additives. The reduction of the porosity is expected to be of advantage for the mechanical properties. The increased amount of the secondary phases possibly affects the irradiation resistance of the joint, but the effects are currently not clear, because both encouraging and negative results were reported. Excellent irradiation-resistance of the pressurized TEP joints was demonstrated following neutron irradiation at 500 and 800°C to up to 5.0 dpa [2]. On the other hand, significant degradation of the strength of monolithic SiC ceramics fabricated by the TEP method was reported following irradiation at 830 and 1270°C to ~6dpa [6]. The possible mechanism of this degradation is cracking and/or strain due to the differential swelling between SiC and the secondary phases. The effects of the secondary phases on the irradiation resistance will be determined in future HFIR irradiation experiment.

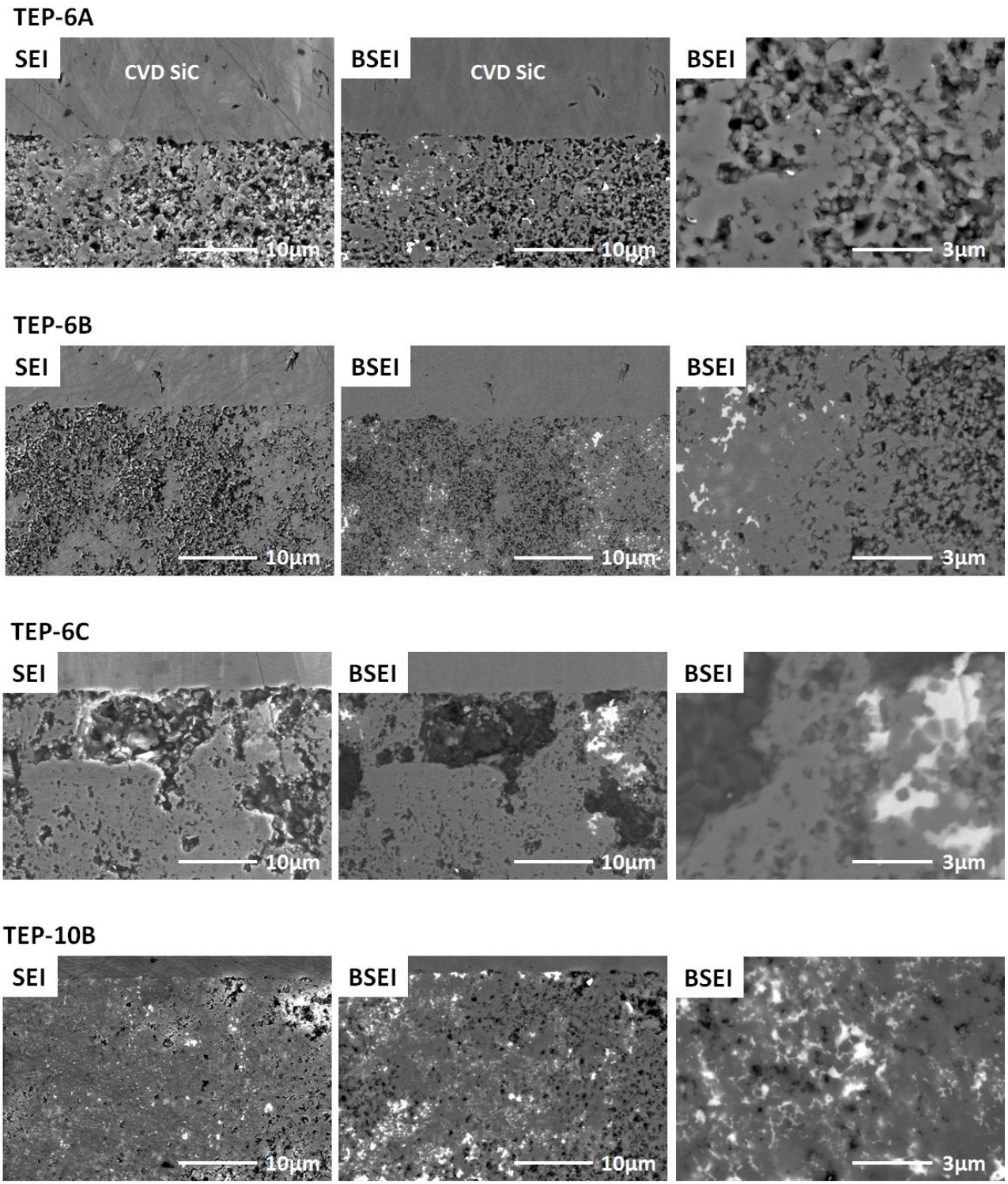

Fig. 8. Secondary electron image (SEI) and backscattered electron image (BSEI) of as-fabricated TEP jointed SiC.

The apparent DNS strengths of 113 MPa and 163 MPa were demonstrated for the TEP-6A and TEP-6B joint specimens, respectively. The one standard deviation was ~50 MPa for both joints. Though the strengths were similar to each other considering the large deviations, obvious difference of the fracture appearance was observed as shown in Figure 9. The TEP-6A joint failed at boned zone by the DNS test. By contrast, cracks ran thorough the SiC substrates in the TEP-6B joint. The failure at the joint in the TEP-6A specimen indicates that the defects in the bonded zone affected this fracture behavior. The DNS strength of ~150 MPa with the failure at the substrates in the TEP-6B specimen is typical for very strong joints, implying absence of severe processing defect or misfit strain at the bonded zone.

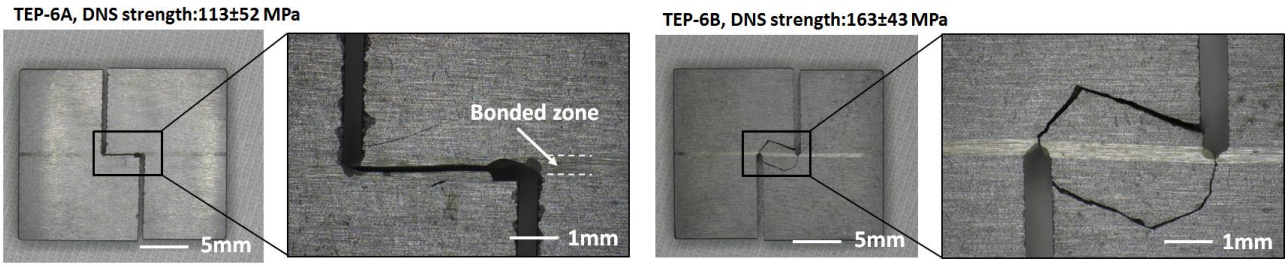

Fig. 9. Optical microscope images of the TEP-6M and TEP-6N specimen after the DNS test. The average strength and the one standard deviation are also shown.

Irradiation test plans

It is planned that rabbit capsules containing the SiC joint specimens are irradiated in HFIR to study effects of irradiation on the shear strength. The conditions planned are irradiation at ~500°C to ~3dpa, ~500°C to >~10 dpa, and ~1000°C to ~3 dpa. The torsional test will be conducted as a post-irradiation experiment. Proven geometries of miniature torsion specimen are adopted in this experiment as shown in Figure 10 [2].

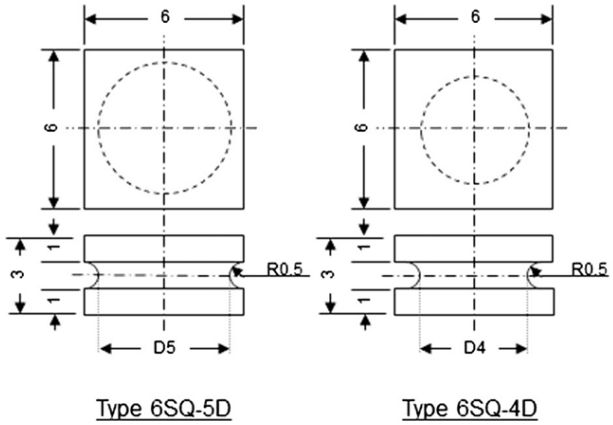

Fig. 10. Geometries of miniature torsion specimens for the irradiation study.

In the previous study conducted as a part of the ORNL and international fusion materials research and development program, several variations of SiC joints were neutron-irradiated in HFIR nominally at 500 and 800ºC to the maximum dose of ~5 dpa. The joint materials included the monolithic SiC and its composites, joined by the titanium diffusion bonding, calcia-alumina (CA) glass-ceramic joining, Ti-Si-C MAX phase joining, TEP slurry joining, and TEP green tape joining. The post-irradiation examination for this experiment showed encouraging results including the retention of the pre-irradiation strength following all irradiation conditions [2]. The new experiment will evaluate irradiation tolerance of additional SiC joints prepared in this work or by collaborators. Effects of temperature and fluence on the irradiation resistance of the SiC joints will be also investigated. The joint materials that are planned to be irradiated in this campaign are listed in Table 2.

Table 2. Candidate materials for irradiation

Material description	Supplier
Rolls-Royce HTC Proprietary, Pressureless MAX-phase	Rolls-Royce HTC/ORNL
Ti Diffusion Bonding	ORNL
Mo Diffusion Bonding	ORNL
Pressureless TEP	ORNL
TEP, Slurry	Kyoto University
TEP, Green Tape	Kyoto University
Calcia-Alumina Glass-Ceramics	Politecnico di Torino
MAX-phase, Green Tape	PNNL
Spark Plasma Sintering	Queen Mary Univ.

REFERENCES

[1] Y. Katoh, L. L. Snead, C. H. Henager Jr, A. Hasegawa, A. Kohyama, B. Riccardi, and H. Hegeman, *J. Nucl. Mater*. **367** (2007) 659.

[2] Y. Katoh, L. L. Snead, T. Cheng, C. Shih, W. D. Lewis, T. Koyanagi, T. Hinoki, C. H. Henager Jr., and M. Ferraris, *J. Nucl. Mater*. (2013) http://dx.doi.org/10.1016/j.jnucmat.2013.10.002.

[3] T. Koyanagi, J. O. Kiggans, T. Cheng, Y. Katoh, Fusion Materials Semiannual Progress Report for Period Ending June 30, 2013, DOE/ER-0313/54, U. S. Department of Energy, 81.

[4] W. J. J. Wakelkamp, F. J. J. van Loo, and R. Metselaar, J. Eur. Ceram. Soc. **8** (1991) 135.

[5] M. W. Barsoum, T. El-Raghy, C. J. Rawn, W. D. Porter, H. Wang, E. A. Payzant, and C. R. Hubbard, *J. Phys. Chem. Solids* **60** (1999) 429.